PROCEEDINGS OF SCIENCE

Twist-3 axial GPDs of the proton from lattice QCD

Martha Constantinou,[a,*] **Shohini Bhattacharya,**[a,b] **Krzysztof Cichy,**[c] **Jack Dodson,**[a] **Andreas Metz,**[a] **Fernanda Steffens**[d] **and Aurora Scapellato**[a]

[a] *Temple University, Philadelphia, PA 19122-1801, USA*

[b] *RIKEN BNL Research Center, Brookhaven National Laboratory, Upton, NY 11973, USA*

[c] *Faculty of Physics, Adam Mickiewicz University, ul. Uniwersytetu Poznańskiego 2, 61-614 Poznań, Poland*

[d] *Insitut für Strahlen- und Kernphysik, Rheinische Friedrich-Wilhelms-Universität Bonn, Nussallee 14-16, 53115 Bonn, Germany*

E-mail: marthac@temple.edu

In these proceedings, we summarize results from the first lattice-QCD calculation of the twist-3 axial quark GPDs for the proton using the large-momentum effective theory approach. The calculation is performed using one $N_f = 2 + 1 + 1$ ensemble of maximally twisted mass fermions with a clover term, that has a volume $32^3 \times 64$, lattice spacing 0.0934 fm, and a pion mass of 260 MeV. The momentum boost of the nucleon matrix elements is 0.83, 1.25, and 1.67 GeV, and the 4-vector momentum transfer squared is 0.69, 1.38, and 2.76 GeV^2. We perform a number of consistency checks, such as the Burkhardt-Cottingham-type as well as Efremov-Teryaev-Leader-type sum rules.

The 40th International Symposium on Lattice Field Theory (Lattice 2023)
July 31st - August 4th, 2023
Fermi National Accelerator Laboratory

*Speaker

PoS(LATTICE2023)315

1. Introduction

Distribution functions of partonic content are key quantities for decoding hadron structure and are categorized in parton distribution functions (PDFs), generalized parton distributions (GPDs), and transverse-momentum-dependent distributions (TMDs). All these distribution functions are classified according to their twist, that is the order of a $1/Q$-expansion they appear in (Q: hard scale of physical process). The leading ones are the twist-2 contributions, while twist-3 is sub-leading. While the latter have been studied very little, they are important for a number of reasons [1]. Thus, they cannot be disregarded, and this work makes an effort to provide information on the twist-3 axial GPDs for the proton, which are interesting in their own right besides assisting in refining the extraction of the twist-2 counterparts. For example, some twist-3 GPDs are related to the orbital angular momentum of quarks, and some provide information about the transverse force acting on a quark in a polarized nucleon.

Direct calculations of GPDs in lattice QCD are not possible due to their light-cone definition. However, the development of modern approaches for accessing GPDs in momentum (x) space has been initiated in recent years. In this study, we employ the quasi-distributions method [2], which utilizes matrix elements with momentum-boosted hadrons coupled to non-local operators containing a straight Wilson line connecting the spatially separated fields. These matrix elements are functions of the length of the Wilson line, z, and can be Fourier transformed in momentum space resulting the quasi-GPDs. Finally, the lattice data are connected to the light-cone GPDs through the framework of Large-Momentum Effective Theory (LaMET) [3]. Extensive reviews of the quasi-distribution approach, along with other methods for obtaining x-dependent distribution functions, can be found in Refs. [4–8].

In the current work, we utilize our experience on the twist-3 proton PDFs, $e(x)$, $g_T(x)$ and $h_L(x)$ [9–12], as well as lattice calculations of twist-2 GPDs conducted by members of our group and collaborators [13, 14], to extract the chiral-even twist-3 axial GPDs. This calculation is quite challenging both computationally and theoretically due to increased gauge noise (momentum boost, momentum transfer, non-local operators), the cost (increased number of matrix elements and number of GPDs, choice of frame), and the enhancement of systematic uncertainties (finite-volume and discretization effects, non-uniqueness of quasi-GPDs definition).

All the above considerations are a significant motivation for exploring lattice-QCD calculations of twist-3 GPDs, a task that is highly demanding but holds tremendous promise for providing valuable insights into these quantities.

2. Theoretical and Computational Setup

Due to space limitations, here we provide a brief summary of the theory and methodology. More details, including the definition of twist-3 GPDs, as well as the parametrization of the matrix elements, can be found in Ref. [1]. To access twist-3 axial GPDs, the relevant operator contains a Dirac structure of $\gamma^j\gamma_5$, where j is perpendicular to the momentum boost, that is, $j = 1, 2$. At the twist-3 level, there are four GPDs. Here, we use a basis for the parametrization that follows

Ref. [15]. Written in coordinate space for the quasi-GPDs (finite momentum boost), one obtains

$$F^{[\gamma^j\gamma_5]}(x,\Delta;P^3) = \frac{\bar{u}(p_f,\lambda')}{2P^3}\Big[\Delta_\perp^j \frac{\gamma_5}{2m} F_{\widetilde{E}+\widetilde{G}_1}(x,\xi,t;P^3) + \gamma_\perp^j\gamma_5 F_{\widetilde{H}+\widetilde{G}_2}(x,\xi,t;P^3) + \Delta_\perp^j \frac{\gamma^3\gamma_5}{P^3} F_{\widetilde{G}_3}(x,\xi,t;P^3) + i\varepsilon_\perp^{j\nu}\Delta_\nu \frac{\gamma^3}{P^3} F_{\widetilde{G}_4}(x,\xi,t;P^3)\Big] u(p_i,\lambda)\,, \quad (1)$$

where F_X denotes quasi-GPDs. The twist-2 GPDs $\widetilde{H}$ and $\widetilde{E}$ also enter the decomposition along with the purely twist-3 ones, $\widetilde{G}_i$ ($i = 1,2,3,4$). We note that the forward limit of the matrix element gives the combination $F_{\widetilde{H}+\widetilde{G}_2} \equiv g_T$, the 2-parton twist-3 PDF that we calculated in Ref. [9]. Different parameterizations for twist-3 light-cone GPDs are available in the literature [16, 17]; see also Ref. [18] where the relations between several definitions can be found.

Exploitation of the symmetry properties of GPDs in position space is of practical value in this calculation, as we can increase statistics by appropriately combining data at the same $|P_3|$, $|z|$, and $-t$. We find that the real part satisfies $\widetilde{G}_1(-P^3) = +\widetilde{G}_1(P^3)$, $\widetilde{G}_2(-P^3) = +\widetilde{G}_2(P^3)$, $\widetilde{G}_3(-P^3) = -\widetilde{G}_3(P^3)$, and $\widetilde{G}_4(-P^3) = +\widetilde{G}_4(P^3)$ ($\widetilde{H}(-P^3) = +\widetilde{H}(P^3)$ and $\widetilde{E}(-P^3) = +\widetilde{E}(P^3)$). Also, $\widetilde{G}_1(-z^3) = +\widetilde{G}_1(z^3)$, $\widetilde{G}_2(-z^3) = +\widetilde{G}_2(z^3)$, $\widetilde{G}_3(-z^3) = -\widetilde{G}_3(z^3)$, and $\widetilde{G}_4(-z^3) = +\widetilde{G}_4(z^3)$ ($\widetilde{H}(-z^3) = +\widetilde{H}(z^3)$ and $\widetilde{E}(-z^3) = +\widetilde{E}(z^3)$). From the combination of hermiticity and time-reversal we find that $\widetilde{G}_1$, $\widetilde{G}_2$, and $\widetilde{G}_4$ exhibit even behavior under $\xi \to -\xi$ ($\widetilde{H}$ and $\widetilde{E}$ are even [19]), while $\widetilde{G}_3$ exhibits odd behavior. Finally, from the requirement of a well-defined forward limit for the matrix elements, it can be shown that $\widetilde{G}_3$ should exhibit at least linear scaling with respect to ξ and without a pole at $\xi = 0$. This is very impactful, as in our $\xi = 0$ calculation, we expect that $\widetilde{G}_3$ is zero.

Here, we use the LaMET approach, which is based on matrix elements of non-local fermion operators where the fermion fields are spatially separated in the $\hat{z}$ direction. The momentum boost is in the same direction as the Wilson line, P_3. Here, we calculate off-forward matrix elements with the direction of the momentum transfer perpendicular to P_3, $\vec{\Delta} = (\Delta_x, \Delta_y, 0)$, corresponds to zero skewness, $\xi = 0$. For the twist-3 axial GPDs, we construct the matrix elements

$$h_j(\Gamma_\kappa, z, p_f, p_i, \mu) = Z_{\gamma_j\gamma_5}(z,\mu)\langle N(p_f)|\overline{\psi}(z)\,\gamma_j\,\gamma_5\,\mathcal{W}(z,0)\psi(0)|N(p_i)\rangle\,, \quad j = 1,\,2\,. \quad (2)$$

The calculation is performed in the symmetric frame corresponding to $\vec{p}_f = \vec{P} + \frac{\vec{\Delta}}{2}$ and $\vec{p}_i = \vec{P} - \frac{\vec{\Delta}}{2}$. We note that a novel method to extract twist-2 GPDs from any kinematic frame via a Lorentz-covariant decomposition has been proposed [20, 21]. The GPDs depend on the 4-vector momentum transfer squared, $-t \equiv \vec{\Delta}^2 - (E_f - E_i)^2$, where E_i and E_f are the energies of the initial and final state ($E_{i/f} = \sqrt{m^2 + \vec{p}^{\,2}_{i/f}}$). $Z_{\gamma_j\gamma_5}$ indicates the renormalization function for the operators and is calculated non-perturbatively [1] using the momentum source method [22, 23] in the modified $\overline{\text{MS}}$ ($\text{M}\overline{\text{MS}}$) scheme [24] at a scale of 2 GeV. Note that the matched (light-cone) GPDs are be converted to the standard $\overline{\text{MS}}$ scheme at 2 GeV through the matching formalism. The parity projector, Γ_κ, entering h_j is chosen to be the unpolarized and three polarized cases defined as $\Gamma_0 = \frac{1}{4}\left(\hat{1} + \gamma^0\right)$, $\Gamma_k = \frac{1}{4}\left(\hat{1} + \gamma^0\right) i\gamma^5\gamma^k$, with $k = 1,\,2,\,3$. Thus, we obtain four independent matrix elements that can disentangle the four twist-3 GPDs through

$$h_j = C\,\text{Tr}\Big[\Gamma_\kappa \left(\frac{-i\not{p}_f + m}{2m}\right) \mathcal{F}^{[\gamma_j\gamma_5]} \left(\frac{-i\not{p}_i + m}{2m}\right)\Big]\,, \quad (3)$$

where $\mathcal{F}^{[\gamma_j\gamma_5]}$ is the $[\cdots]$ component of Eq. (1) written in Euclidean space. The kinematic factor C in the symmetric frame at zero skewness reads $C = \frac{2m^2}{E(E+m)}$ ($E_i = E_f \equiv E$).

The position-space quasi-GPDs, $F_X(z)$, are transformed in momentum space, $F_X(x)$, defined through a Fourier transform. The lattice discretization and periodicity lead to a small set of values for z in the range $[0, L/2]$ (L: spatial extent of lattice). This so-called inverse problem in the reconstruction of the x-dependence does not have a unique solution. Here, we use the model-independent Backus-Gilbert reconstruction method [25], which we implement according to Ref. [26]. The quasi-GPDs are connected to their light-cone counterparts through the matching formalism. The matching kernel, C_X, is calculated order by order in perturbation theory and, at one-loop for zero skewness, reads

$$F_X^{\overline{\rm MMS}}(x,t,P_3,\mu) = \int_{-1}^{1} \frac{dy}{|y|} C^{\overline{\rm MMS},\overline{\rm MS}}_{\gamma_j\gamma_5}\left(\frac{x}{y}, \frac{\mu}{yP_3}\right) G_X^{\overline{\rm MS}}(y,t,\mu) \; + O\left(\frac{m^2}{P_3^2}, \frac{t}{P_3^2}, \frac{\Lambda^2_{\rm QCD}}{x^2P_3^2}\right). \quad (4)$$

At $\xi = 0$, C_X is expected to coincide with its forward limit [27] given in Ref. [10]. C_X is the same for $\widetilde{H} + \widetilde{G}_2$, $\widetilde{E} + \widetilde{G}_1$, $\widetilde{G}_3$, and $\widetilde{G}_4$ because they are extracted from the same operator.

In this calculation, we use one ensemble of two $N_f = 2 + 1 + 1$ twisted mass fermions with a cover term [28], where the mass of the light quarks has been tuned to produce a pion mass of 260 MeV. The lattice spacing is $a \simeq 0.093$ fm, and the lattice volume is $32^3 \times 64$ ($L \approx 3$ fm).

The construction of the matrix element h_j combines the proton two-point and three-point correlation functions. For the latter, we use the sequential method that requires fixing the source-sink time separation, t_s, but allows one to obtain the matrix element for any operator at a very small additional computational cost. In this work, we choose $t_s = 10a$ to control statistical uncertainties and focus on the $u - d$ isovector flavor combination. Thus, the disconnected contribution of $u - d$ is safely neglected. h_j denotes the ground-state contribution of an appropriate ratio between the 2pt- and 3pt- functions that cancels the time dependence of the exponentials introduced by the non-zero momentum transfer between the initial and final states, as well as the overlap from the interpolating fields. The ground-state matrix elements are obtained from a plateau fit with respect to operator insertion time in a region of convergence, indicated by $\Pi^j(\Gamma_\kappa)$.

We calculate h_j for a class of momenta of the form $\vec{\Delta} = (\pm q, 0, 0)$, $\vec{\Delta} = (0, \pm q, 0)$, and $\vec{\Delta} = (\pm q, \pm q, 0)$ leading to $-t = 0$, 0.69, 1.38, 2.76 GeV^2. These are combined with $\pm P_3 =$ 0.83, 1.25, 1.67 GeV. Overall, the various combinations of $\pm$ momenta lead to a factor of eight more statistics. An additional factor of two in the number of matrix elements comes from averaging the matrix elements h_1 and h_2. A large number of statistics is required for the high values of P_3 and $-t$, and here we use $O(10^3) - O(10^5)$ measurements. The exact statistics can be found in Ref. [1].

3. Results

In Fig. 1, we show some representative matrix elements for $\vec{\Delta} = \pm\frac{2\pi}{L}(2, 0, 0)$ plus permutations and $P_3 = \pm 1.25$ GeV ($-t = 0.69$ GeV^2). The data correspond to h^j projected by Γ_j, while the momentum transfer in the j direction is zero. The matrix elements have definite symmetry properties for the various $\pm P_3$, $\pm z$, and $\pm\vec{\Delta}$ cases. As can be seen, the real part is fully symmetric, while the imaginary part is symmetric in $\pm\vec{\Delta}$, but anti-symmetric in $P \cdot z$. We note that the matrix

element related to $\widetilde{G}_3$ is compatible with zero, a conclusion that holds for all values of $-t$ we explore here. This behavior is due to the zero skewness calculation (see, e.g., Eq. (6)).

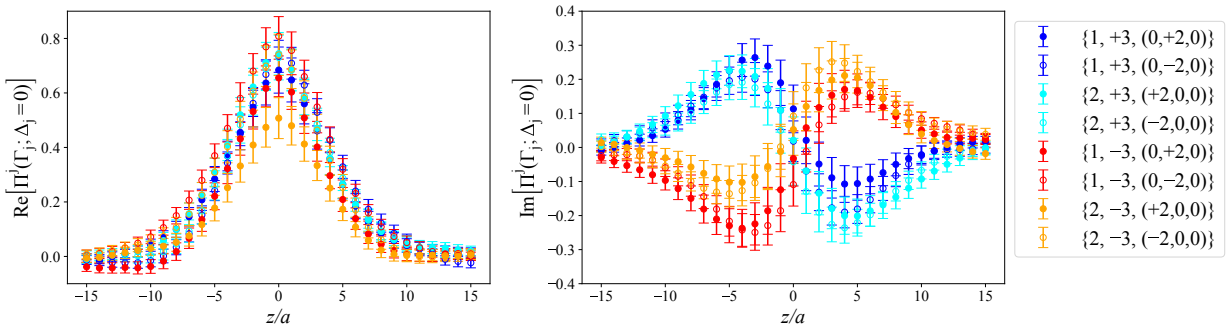

Figure 1: Real (left) and imaginary (right) parts of the matrix elements $\Pi^j(\Gamma_j)$ for all kinematic cases corresponding to $\Delta_j = 0$ at $-t = 0.69$ GeV^2 and $|P_3| = 1.25$ GeV. The data are indicated by $\{j, P_3, \vec{\Delta}\}$, where $P_3 = \pm 3$, and $\vec{\Delta} = (\pm 2, 0, 0),\ (0, \pm 2, 0)$. The momenta are given in units of $\frac{2\pi}{L}$.

Using all independent matrix elements we decompose the quasi-GPDs in position space, $F_X(z)$ where $X = \widetilde{H} + \widetilde{G}_2,\ \widetilde{E} + \widetilde{G}_1,\ \widetilde{G}_3,\ \widetilde{G}_4$. We examine the P_3 and $-t$ dependence independently on the numerically dominant GPDs $F_{\widetilde{H}+\widetilde{G}_2}$ and $F_{\widetilde{E}+\widetilde{G}_1}$. The former can be found in Ref. [1] for $-t = 0.69$ GeV^2, for which have $P_3 = 0.83,\ 1.25,\ 1.67$ GeV. For $F_{\widetilde{H}+\widetilde{G}_2}$, we find a mild P_3 dependence, while a more noticeable P_3 dependence is observed in $F_{\widetilde{E}+\widetilde{G}_1}$. The dependence of F_X on the momentum

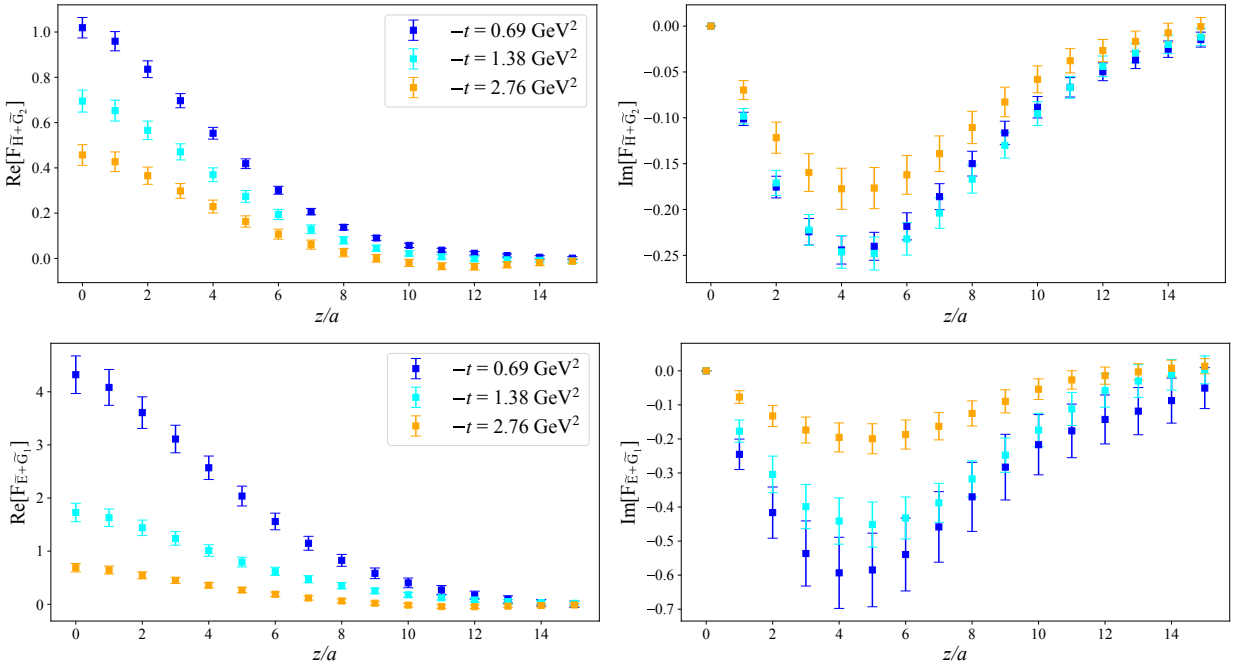

Figure 2: Real (left) and imaginary (right) parts of $F_{\widetilde{H}+\widetilde{G}_2}$ (top) and $F_{\widetilde{E}+\widetilde{G}_1}$ (bottom) at $P_3 = 1.25$ GeV and $-t = 0.69,\ 1.38,\ 2.76$ GeV^2. All kinematically equivalent cases have been averaged. The errors correspond to the statistical uncertainties.

transfer is shown in Fig. 2, where the momentum boost is fixed to $|P_3| = 1.25$ GeV. We find a smooth $-t$ behavior and, in particular, a decrease in the magnitude of F_X as $-t$ increases. Another

general finding is that $F_{\widetilde{E}+\widetilde{G}_1}$ is noisier than $F_{\widetilde{H}+\widetilde{G}_2}$, as well as larger in magnitude. This is expected from the behavior of the axial, G_A, and induced pseudoscalar, G_P, form factors [29], which are related to the above-mentioned quantities through the generalization of Burkhardt-Cottingham sum rules [15, 30] and the zero norm of $\widetilde{G}_i$,which also holds for quasi-GPDs.

$$\int_{-1}^{1} dx\, \widetilde{H}(x,\xi,t) = G_A(t)\,, \quad \int_{-1}^{1} dx\, \widetilde{E}(x,\xi,t) = G_P(t)\,, \quad \int_{-1}^{1} dx\, \widetilde{G}_i(x,\xi,t) = 0\,,\ i = 1-4\,, \quad (5)$$

Finally, the noise increase becomes more prominent for the large values of $-t$, even though there is a good signal for all cases and a hierarchy among the various momentum transfers, where the quasi-GPDs are decaying towards zero as $-t$ increases. The difference between $-t = 0.69$ GeV^2 and $-t = 1.38$ GeV^2 is very small for the imaginary part of both $F_{\widetilde{H}+\widetilde{G}_2}$ and $F_{\widetilde{E}+\widetilde{G}_1}$.

As mentioned previously, $F_{\widetilde{G}_3}$ is zero for $\xi = 0$, which is consistent with the generalization of the Efremov-Leader-Teryaev sum rules [31]

$$\int dx\, x\, \widetilde{G}_3 = \frac{\xi}{4} G_E(t)\,. \quad (6)$$

$F_{\widetilde{G}_4}$, is found to be small but not negligible, as depicted by the sum rule connecting it to the electric Sachs form factor G_E,

$$\int_{-1}^{1} dx\, x\, \widetilde{G}_4(x,\xi,t) = \frac{1}{4} G_E\,. \quad (7)$$

Due to space limitation, we will only show the light-cone $\widetilde{G}_4$ below.

The quasi-GPDs in position space are used to reconstruct the x-dependence of the light-cone GPDs, for which we use the Backus-Gilbert method on each F_X and then apply the matching kernel to obtain the light-cone GPDs as a function of x. Since we perform the calculation at zero skewness, it is anticipated that the matching formalism of GPDs is the same as for PDFs [27]. Thus, we use the results of Ref. [10], which correspond to the forward limit of the twist-3 axial GPDs, g_T. A dedicated analytic calculation for the twist-3 case is required to prove this argument, which we leave as future work. In this presentation, we neglect $\widetilde{G}_3$, which was found to be zero. We have examined the dependence of the quasi-GPDs on the maximum value of z that enters the Backus-Gilbert reconstruction, with $z_{\rm max} = 9a$, $11a$, $13a$. We consistently find that $z_{\rm max} = 11a$ is optimal for all cases, and we include a systematic error equal to one-half of the difference of the results between $z_{\rm max} = 9a$ and $z_{\rm max} = 13a$ to reflect the uncertainty in the choice of $z_{\rm max}$.

The P_3-dependence of the final matched (light-cone) GPDs has been explored and is presented in Ref. [1] for $-t = 0.69$ GeV^2. We find that both $\widetilde{H} + \widetilde{G}_2$ and $\widetilde{E} + \widetilde{G}_1$ have mild P_3 dependence in the region $x \in [0, 0.4]$. We observe some differences in the region $x \in [0.5, 0.7]$, while the above-mentioned GPDs at different P_3 values converge to the same function in the large x region. Regarding $\widetilde{G}_4$, the P_3 behavior is very similar for the $-1 < x < 0.4$ region. For larger values of x, some differences are observed. Nevertheless, the convergence in P_3 is satisfactory within the reported uncertainties.

Fig. 3 shows the $-t$ dependence of $\widetilde{H} + \widetilde{G}_2$ and $\widetilde{E} + \widetilde{G}_1$ for the available values of $-t = 0.69, 1.38, 2.76$ GeV^2. As $-t$ increases, the GPDs decrease in value for the region $x \in [0, 0.8]$. On the contrary, the large-x region is not very sensitive to $-t$. Also, the $-t$ dependence is more prominent in $\widetilde{E} + \widetilde{G}_1$ compared to $\widetilde{H} + \widetilde{G}_2$. This could be an indication of the pion pole expected in

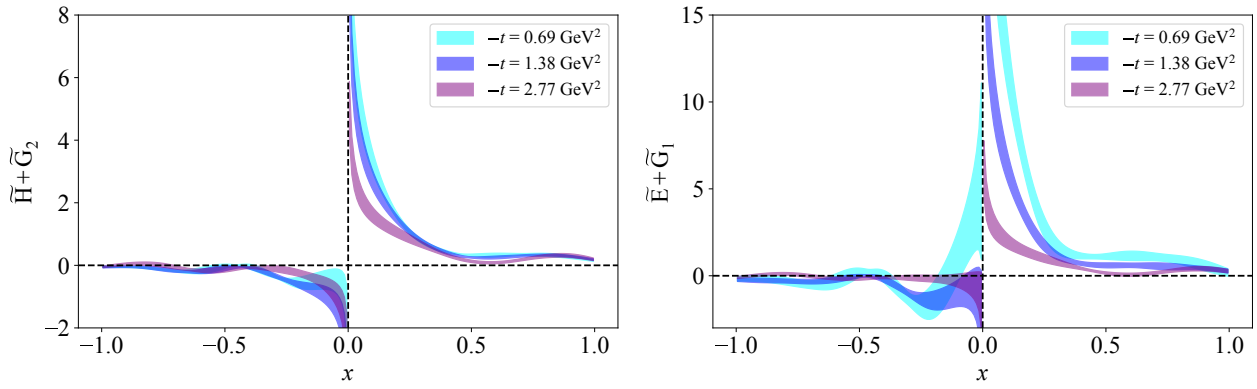

Figure 3: $\widetilde{H}+\widetilde{G}_2$ (left) and $\widetilde{E}+\widetilde{G}_1$ (right) and $P_3 = 1.25$ GeV for various values of $-t$. Results are given in the $\overline{\text{MS}}$ scheme at a scale of 2 GeV. The bands correspond to the statistical errors and the systematic uncertainty due to the x-dependent reconstruction.

$\widetilde{E}$ [32], which requires further investigation, including data at nonzero skewness. The $-t$ dependence of $\widetilde{G}_4$ is shown in Fig. 4 and has similar behavior as $\widetilde{H}+\widetilde{G}_2$ and $\widetilde{E}+\widetilde{G}_1$.

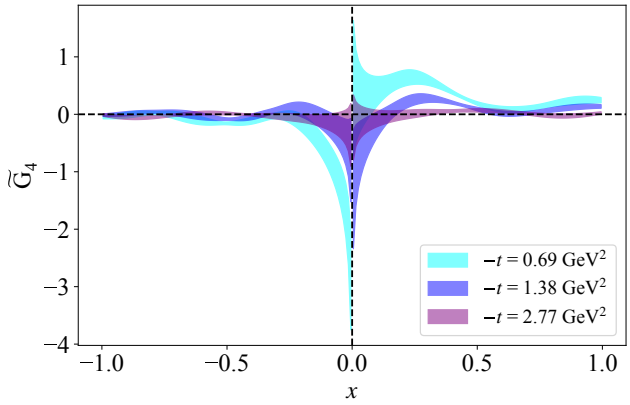

Figure 4: $\widetilde{G}_4$ at $P_3 = 1.25$ GeV for various values of $-t$. Results are given in the $\overline{\text{MS}}$ scheme at a scale of 2 GeV. The bands correspond to the statistical errors and the systematic uncertainty due to the x-dependent reconstruction.

Another aspect of this work is to isolate $\widetilde{G}_2$ by combining our results on $\widetilde{H}+\widetilde{G}_2$ from the twist-3 ($\gamma_j\gamma_5$) calculation and $\widetilde{H}$ from the twist-2 ($\gamma_3\gamma_5$) calculation. We extracted both quantities on the same configurations and kinematical setup, which makes it possible to isolate $\widetilde{G}_2$. The $-t$ dependence is shown in the left panel of Fig. 5, which appears to be non-monotonic. Also, it is observed that $\widetilde{G}_2$ becomes negative in the intermediate positive x region. We anticipate that this behavior is not unphysical as the norm of both the quasi and light-cone $\widetilde{G}_2$ should vanish, indicating that negative regions must exist. It is interesting to compare $\widetilde{H}+\widetilde{G}_2$, $\widetilde{H}$, and $\widetilde{G}_2$. These quantities are shown in the right panel of Fig. 5 at $-t = 0.69$ GeV^2. The difference between $\widetilde{H}+\widetilde{G}_2$ and $\widetilde{H}$ is large, which leads to a sizeable $\widetilde{G}_2$.

A similar analysis of extracting $\widetilde{G}_1$ is only possible at nonzero skewness because $\widetilde{E}$ has a vanishing kinematic factor at $\xi = 0$ in the parametrization of the twist-2 matrix element $\gamma_3\gamma_5$. This gives a high value of the twist-3 calculation, as it provides information on $\widetilde{E}$ through its twist-3

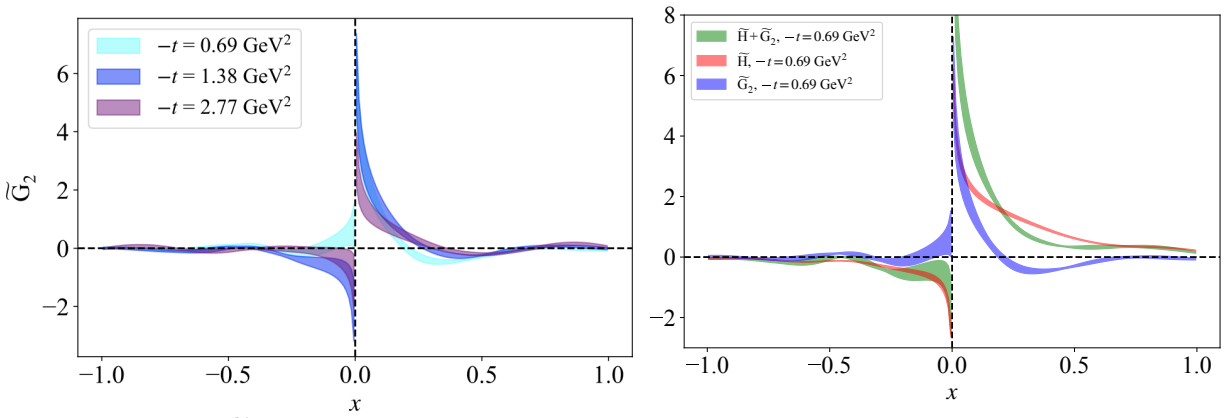

Figure 5: Left: $\widetilde{G}_2$ at $P_3 = 1.25$ GeV and various $-t$. Results are given in the $\overline{\text{MS}}$ scheme at a scale of 2 GeV. Right: Comparison of $\widetilde{H}$, $\widetilde{H}+\widetilde{G}_2$, and $\widetilde{G}_2$ at $-t = 0.69$ GeV^2. Results are given in the $\overline{\text{MS}}$ scheme at a scale of 2 GeV. All bands correspond to the statistical errors and the systematic uncertainty due to the x-dependent reconstruction.

counterpart, $\widetilde{E}+\widetilde{G}_1$. In addition, one can also extract the Mellin moments of $\widetilde{E}$ directly from the twist-3 data using the sum rule of Eq. (5) combined with the fact that the integral of G_1 is zero (see, Eq. (5)).

A number of consistency checks have been performed, which include the local limit of twist-3 GPDs, their norms, and the P_3 independence of the norms. The outcome is very encouraging, but further investigation is needed to provide quantitative results, e.g., the Mellin moments. More detailed discussion can be found in Ref. [1].

4. Summary

In this study, we present results on the axial twist-3 GPDs, $\widetilde{H}+\widetilde{G}_2$, $\widetilde{E}+\widetilde{G}_1$, $\widetilde{G}_3$, and $\widetilde{G}_4$. We employ the quasi-distributions method, allowing access to the x-dependence of GPDs, necessitating the evaluation of matrix elements of nonlocal operators and momentum-boosted hadrons. Our approach employs the axial-vector operator with spatial indices perpendicular to the boost direction, corresponding to the twist-3 counterpart of the helicity GPD.

The computations are performed in the symmetric frame, which is computationally intensive and requires separate calculations for each momentum transfer value, $-t$. We obtain results at zero skewness and for three values, $-t = 0.69$, 1.38, and 2.76 GeV^2 at momentum boost $P_3 = 1.25$ GeV. Convergence checks in P_3 at $-t = 0.69$ GeV^2 are performed for three values, namely $P_3 = 0.83$, 1.25, and 1.67 GeV.

Our analysis employs the unpolarized and three polarized parity projectors, yielding four independent matrix elements that successfully disentangle the four twist-3 GPDs. Notably, $\widetilde{H}+\widetilde{G}_2$ and $\widetilde{E}+\widetilde{G}_1$ exhibit a robust signal for all P_3 and $-t$ values. In contrast, $\widetilde{G}_4$ is smaller in magnitude with a higher relative error. $\widetilde{G}_3$ is compatible with zero due to the calculation at zero skewness.

An additional component of the calculation is the extraction of $\widetilde{G}_2$ by combining $\widetilde{H}+\widetilde{G}_2$ with the twist-2 $\widetilde{H}$ GPD. This analysis reveals intriguing features, such as negative values for $\widetilde{G}_2$ at the intermediate range of x, justified by the expectation of a zero norm for $\widetilde{G}_2$.

Despite the increased noise-to-signal ratios for the matrix elements of operators $\gamma_1\gamma_5$ and $\gamma_2\gamma_5$ compared to the twist-2 case $\gamma_3\gamma_5$, our results demonstrate that a momentum boost of $P_3 = 1.25$ GeV is adequate for matching lattice data to light-cone GPDs. We highlight that this marks the first lattice QCD calculation of twist-3 GPDs, and therefore, there are sources of systematic uncertainties to be addressed, such as excited states effects, uncertainties related to the momentum boost, and the mixing between two-parton and three-parton correlators. Our future work will address some of these systematics and also explore the Wandzura-Wilczek approximation intricacies. In addition to the study of the axial twist-3 GPDs, we will also extend our calculations to other cases, that is, the scalar, vector, and tensor twist-3 GPDs.

Acknowledgements

The authors are grateful to Joshua Miller for helping in the presentation of results in the manuscript. S. B. has been supported by the U.S. Department of Energy under Contract No. DE-SC0012704, and also by Laboratory Directed Research and Development (LDRD) funds from Brookhaven Science Associates. The work of S.B. and A.M. has been supported by the National Science Foundation under grant number PHY-2110472. A.M. has also been supported by the U.S. Department of Energy, Office of Science, Office of Nuclear Physics, within the framework of the TMD Topical Collaboration. K.C. is supported by the National Science Centre (Poland) grants SONATA BIS no. 2016/22/E/ST2/00013 and OPUS no. 2021/43/B/ST2/00497. M.C., J.D. and A.S. acknowledge financial support by the U.S. Department of Energy, Office of Nuclear Physics, Early Career Award under Grant No. DE-SC0020405. F.S. was funded by the NSFC and the Deutsche Forschungsgemeinschaft (DFG, German Research Foundation) through the funds provided to the Sino-German Collaborative Research Center TRR110 "Symmetries and the Emergence of Structure in QCD" (NSFC Grant No. 12070131001, DFG Project-ID 196253076 - TRR 110). We acknowledge partial support by the U.S. Department of Energy, Office of Science, Office of Nuclear Physics under the Quark-Gluon Tomography (QGT) Topical Collaboration with Award DE-SC0023646. Computations for this work were carried out in part on facilities of the USQCD Collaboration, which are funded by the Office of Science of the U.S. Department of Energy. This research was supported in part by PLGrid Infrastructure (Prometheus supercomputer at AGH Cyfronet in Cracow). Computations were also partially performed at the Poznan Supercomputing and Networking Center (Eagle supercomputer), the Interdisciplinary Centre for Mathematical and Computational Modelling of the Warsaw University (Okeanos supercomputer), and the Academic Computer Centre in Gdańsk (Tryton supercomputer). The gauge configurations have been generated by the Extended Twisted Mass Collaboration on the KNL (A2) Partition of Marconi at CINECA, through the Prace project Pra13_3304 "SIMPHYS". Inversions were performed using the DD-αAMG solver [33] with twisted mass support [34].

References

[1] S. Bhattacharya, K. Cichy, M. Constantinou, J. Dodson, A. Metz, A. Scapellato, and F. Steffens, "Chiral-even axial twist-3 GPDs of the proton from lattice QCD," *Phys. Rev. D*, vol. 108, no. 5, p. 054501, 2023.

[2] X. Ji, "Parton Physics on a Euclidean Lattice," *Phys. Rev. Lett.*, vol. 110, p. 262002, 2013.

[3] X. Ji, "Parton Physics from Large-Momentum Effective Field Theory," *Sci. China Phys. Mech. Astron.*, vol. 57, pp. 1407–1412, 2014.

[4] K. Cichy and M. Constantinou, "A guide to light-cone PDFs from Lattice QCD: an overview of approaches, techniques and results," *Adv. High Energy Phys.*, vol. 2019, p. 3036904, 2019.

[5] X. Ji, Y.-S. Liu, Y. Liu, J.-H. Zhang, and Y. Zhao, "Large-momentum effective theory," *Rev. Mod. Phys.*, vol. 93, no. 3, p. 035005, 2021.

[6] M. Constantinou, "The x-dependence of hadronic parton distributions: A review on the progress of lattice QCD," *Eur. Phys. J. A*, vol. 57, no. 2, p. 77, 2021.

[7] K. Cichy, "Progress in x-dependent partonic distributions from lattice QCD," in *38th International Symposium on Lattice Field Theory*, 10 2021.

[8] K. Cichy, "Overview of lattice calculations of the x-dependence of PDFs, GPDs and TMDs," *EPJ Web Conf.*, vol. 258, p. 01005, 2022.

[9] S. Bhattacharya, K. Cichy, M. Constantinou, A. Metz, A. Scapellato, and F. Steffens, "Insights on proton structure from lattice QCD: The twist-3 parton distribution function $g_T(x)$," *Phys. Rev. D*, vol. 102, no. 11, p. 111501, 2020.

[10] S. Bhattacharya, K. Cichy, M. Constantinou, A. Metz, A. Scapellato, and F. Steffens, "One-loop matching for the twist-3 parton distribution $g_T(x)$," *Phys. Rev. D*, vol. 102, no. 3, p. 034005, 2020.

[11] S. Bhattacharya, K. Cichy, M. Constantinou, A. Metz, A. Scapellato, and F. Steffens, "The role of zero-mode contributions in the matching for the twist-3 PDFs $e(x)$ and $h_L(x)$," *Phys. Rev. D*, vol. 102, p. 114025, 2020.

[12] S. Bhattacharya, K. Cichy, M. Constantinou, A. Metz, A. Scapellato, and F. Steffens, "Parton distribution functions beyond leading twist from lattice QCD: The hL(x) case," *Phys. Rev. D*, vol. 104, no. 11, p. 114510, 2021.

[13] C. Alexandrou, K. Cichy, M. Constantinou, K. Hadjiyiannakou, K. Jansen, A. Scapellato, and F. Steffens, "Unpolarized and helicity generalized parton distributions of the proton within lattice qcd," *Phys. Rev. Lett.*, vol. 125, p. 262001, Dec 2020.

[14] C. Alexandrou, K. Cichy, M. Constantinou, K. Hadjiyiannakou, K. Jansen, A. Scapellato, and F. Steffens, "Transversity gpds of the proton from lattice qcd," 2021.

[15] D. V. Kiptily and M. V. Polyakov, "Genuine twist three contributions to the generalized parton distributions from instantons," *Eur. Phys. J. C*, vol. 37, pp. 105–114, 2004.

[16] A. V. Belitsky, D. Mueller, and A. Kirchner, "Theory of deeply virtual Compton scattering on the nucleon," *Nucl. Phys. B*, vol. 629, pp. 323–392, 2002.

[17] S. Meissner, A. Metz, and M. Schlegel, "Generalized parton correlation functions for a spin-1/2 hadron," *JHEP*, vol. 08, p. 056, 2009.

[18] F. Aslan, M. Burkardt, C. Lorcé, A. Metz, and B. Pasquini, "Twist-3 generalized parton distributions in deeply-virtual Compton scattering," *Phys. Rev. D*, vol. 98, no. 1, p. 014038, 2018.

[19] S. Bhattacharya, C. Cocuzza, and A. Metz, "Exploring twist-2 GPDs through quasidistributions in a diquark spectator model," *Phys. Rev. D*, vol. 102, no. 5, p. 054021, 2020.

[20] S. Bhattacharya, K. Cichy, M. Constantinou, J. Dodson, X. Gao, A. Metz, S. Mukherjee, A. Scapellato, F. Steffens, and Y. Zhao, "Generalized parton distributions from lattice QCD with asymmetric momentum transfer: Unpolarized quarks," *Phys. Rev. D*, vol. 106, no. 11, p. 114512, 2022.

[21] S. Bhattacharya *et al.*, "Generalized Parton Distributions from Lattice QCD with Asymmetric Momentum Transfer: Axial-vector case," 10 2023.

[22] M. Gockeler, R. Horsley, H. Oelrich, H. Perlt, D. Petters, P. E. L. Rakow, A. Schafer, G. Schierholz, and A. Schiller, "Nonperturbative renormalization of composite operators in lattice QCD," *Nucl. Phys.*, vol. B544, pp. 699–733, 1999.

[23] C. Alexandrou, M. Constantinou, and H. Panagopoulos, "Renormalization functions for Nf=2 and Nf=4 twisted mass fermions," *Phys. Rev.*, vol. D95, no. 3, p. 034505, 2017.

[24] C. Alexandrou, K. Cichy, M. Constantinou, K. Hadjiyiannakou, K. Jansen, A. Scapellato, and F. Steffens, "Systematic uncertainties in parton distribution functions from lattice QCD simulations at the physical point," *Phys. Rev.*, vol. D99, no. 11, p. 114504, 2019.

[25] G. Backus and F. Gilbert, "The resolving power of gross earth data," *Geophysical Journal International*, vol. 16, no. 2, pp. 169–205, 1968.

[26] C. Alexandrou, K. Cichy, M. Constantinou, K. Hadjiyiannakou, K. Jansen, A. Scapellato, and F. Steffens, "Transversity GPDs of the proton from lattice QCD," *Phys. Rev. D*, vol. 105, no. 3, p. 034501, 2022.

[27] Y.-S. Liu, W. Wang, J. Xu, Q.-A. Zhang, J.-H. Zhang, S. Zhao, and Y. Zhao, "Matching generalized parton quasidistributions in the RI/MOM scheme," *Phys. Rev. D*, vol. 100, no. 3, p. 034006, 2019.

[28] C. Alexandrou *et al.*, "Quark masses using twisted-mass fermion gauge ensembles," *Phys. Rev. D*, vol. 104, no. 7, p. 074515, 2021.

[29] C. Alexandrou *et al.*, "Nucleon axial and pseudoscalar form factors from lattice QCD at the physical point," *Phys. Rev. D*, vol. 103, no. 3, p. 034509, 2021.

[30] X.-D. Ji, "Gauge-Invariant Decomposition of Nucleon Spin," *Phys. Rev. Lett.*, vol. 78, pp. 610–613, 1997.

[31] A. V. Efremov, O. V. Teryaev, and E. Leader, "An Exact sum rule for transversely polarized DIS," *Phys. Rev. D*, vol. 55, pp. 4307–4314, 1997.

[32] M. Penttinen, M. V. Polyakov, and K. Goeke, "Helicity skewed quark distributions of the nucleon and chiral symmetry," *Phys. Rev. D*, vol. 62, p. 014024, 2000.

[33] A. Frommer, K. Kahl, S. Krieg, B. Leder, and M. Rottmann, "Adaptive aggregation-based domain decomposition multigrid for the lattice Wilson–Dirac operator," *SIAM J. Sci. Comput.*, vol. 36, pp. A1581–A1608, 2014.

[34] C. Alexandrou, S. Bacchio, J. Finkenrath, A. Frommer, K. Kahl, and M. Rottmann, "Adaptive aggregation-based domain decomposition multigrid for twisted mass fermions," *Phys. Rev. D*, vol. 94, p. 114509, 2016.